Slope Stability in Open Pits with Thin Weak Layers

Fredy A. Díaz-Durán(✉)

Tecnológico de Monterrey, Monterrey, N.L. 64849, México
fredy.diaz@tec.mx

Abstract. Open pit mining projects usually face particular situations while dealing with slope stability analysis. More than any other projects, mining projects build a considerable number of slopes, which are more likely to behave differently among them, due to the change in orientation in the open pit. One of the situations that represent a considerable problem is the presence of a weak layer, which could be easily analyzed by using the limit equilibrium methods. Nonetheless, there are some practical measures that mining engineers take in order to improve the slope stability condition of mining slopes involving a weak layer, which consist in creating a disturbance in the rock medium surrounding the weak layer by blasting a strip of the rock mass. That modification of the rock medium is not easy to analyze with traditional limit equilibrium methods, because there is not a constitutive model to properly characterize that portion of the disturbed medium. This paper presents a first approach to analyze the stability in open pit mining slopes in the presence of a weak layer, both, before and after blasting to create a disturbance of the medium. This approach considers the effect of the rock mass disturbance, by using a combination between data coming from inclinometer monitoring in the slopes and numerical simulations with finite elements, which allows to monitor the slope stability during the rock mass disturbance. The disturbed rock mass, known as "bimrock", is then characterized and included into the slope stability models to obtain the factor of safety considering the disturbance of the medium.

Keywords: Slope Stability Analysis · Limit Equilibrium Method · Finite Element Method · Slope Monitoring · Bimrock

1 Introduction

1.1 Methods to Assess the Slope Stability

Assessing slope stability is crucial in open pit mining operations, and the most commonly used technique for this purpose is the limit equilibrium method, as excavation work continues. Despite its popularity due to its simplicity, the limit equilibrium method may encounter various computational challenges and numerical inconsistencies when determining the factor of safety. One such limitation is the inability to incorporate data related to deformation or displacements, including information obtained through geotechnical monitoring instruments (e.g. inclinometers, extensometers, etc.).

R. E. Hammah et al. (Eds.): RIC 2023, AHE 19, pp. 522–533, 2023.
https://doi.org/10.2991/978-94-6463-258-3_50

In contrast, the finite element method is an alternative technique for evaluating slope stability. It offers a significant advantage over the limit equilibrium method in that it does not rely on assumptions about the shape or position of the critical failure surface. Furthermore, the finite element method allows for the calculation of stresses and displacements, which is particularly beneficial in monitoring progressive failure.

The comparison of these two techniques has been performed by a number of authors. Now it is clear that the finite element method (FEM) provides tangible benefits over the limiting equilibrium methods, such as the possibility of considering deformations in the analysis [9]; FEM also outstands when dealing with complex geometries and material properties [6]. Additionally, analysis of slopes utilizing both the limit equilibrium method and the limit analysis method are widely reported. For example, some results of these kind of analysis outlined that the outcomes generated by the two approaches were largely consistent only for homogeneous slopes [5]. Another comparison of the outcomes from finite element method and those produced by the limiting equilibrium method, concluded that the finite element method was more practically useful [8]. Another approach corroborates the fact that there are differences between the safety factors obtained through the finite element method and various limiting equilibrium methods [3]. Moreover, it has been highlight that finite element method features an automatic mechanism for determining the critical limit load and conducting associated lower and upper bound analyses, which is regarded as a distinct advantage over the limiting equilibrium method [2].

1.2 Thin and Weak Layers in Open Pit Slopes

The wall design for open pits involves various levels and stages of analysis, encompassing local slope stability examination, overall stability assessment, performance evaluation, and parameter calibration through back-analysis. This process demands an array of analysis methods and software, spanning from limiting equilibrium methods to more intricate numerical analyses such as distinct elements, capable of accommodating mixed failure modes and accounting for intricate geology.

Crusoe, et al. [2] performed an analysis to understand how the angle and thickness of a weak layer can affect the stability of rock slopes. That study examined the impact of weak layers on failure modes and safety factors in rock slopes, finding that an increase in the angle or thickness of the weak layer leads to an expansion of the failure zone and can alter the mode of failure. Thus, by intervening the thin layer it will be possible to reduce that potential failure zone.

2 Site Description

An open pit mining operation was preparing to commence excavation in sequential stages, each one progressing 10 m deeper into the ground and slopes inclined at 70 degrees. The stability assessment of the mining excavation design followed the conventional approach, which involved analyzing potential kinematic mechanisms such as planar and wedge failure. Furthermore, limit equilibrium methods were also utilized for slope stability assessment, however, the use of finite element methods was scarce.

2.1 Geological and Geotechnical Model

A three-layered geological model was proposed for the site, consisting of two lower layers of sandstones and an upper layer of claystone. Additionally, a thin layer of plastic clay, detected during subsoil exploration and measuring close to 0.5 m in thickness, was incorporated in the middle of the upper sandstone layer (see Fig. 1).

In order to evaluate the shear strength properties of the rock mass, results of the uniaxial compressive strength tests conducted on rock cores were used. The failure criterion proposed for this analysis was the one proposed by Hoek and Brown, modified by Carranza-Torres & Corkum [4], which allows for the calculation of equivalent strength parameters (cohesion and friction angle) in rock materials, as it follows:

$$\sigma'_1 = \sigma'_3 + \sigma_{ci}\left(m_b \frac{\sigma'_3}{\sigma_{ci}} + s\right)^{\alpha} \tag{1}$$

where m_b is obtained from the value of the material constant m_i, while s and α are constants of the rock mass. Then, the equivalent parameters can be determined from the following expressions:

$$c' = \frac{\sigma_{ci}[(1+2\alpha)s + (1-\alpha)m_b\sigma'_{3n}](s + m_b\sigma'_{3n})^{\alpha-1}}{(1+\alpha)(2+\alpha)\sqrt{1 + \left(\frac{6\alpha m_b(s+m_b\sigma'_{3n})^{\alpha-1}}{(1+\alpha)(2+\alpha)}\right)}} \tag{2}$$

$$\phi' = \sin^{-1}\left[\frac{6\alpha mb(s + m_b\sigma'_{3n})^{\alpha-1}}{2(1+\alpha)(2+\alpha) + 6\alpha m_b(s + m_b\sigma'_{3n})^{\alpha-1}}\right] \tag{3}$$

For the plastic clay, a direct shear test was performed to obtained the shear strength parameters. The following Table 1 presents the initial geomechanical and elastic properties of the materials included in the model.

In this study, the decision to derive equivalent Mohr-Coulomb parameters characterize rock materials, rather than directly utilizing the rock mass parameters in the software, was made to facilitate comparison between the equivalent rock mass parameters and those used to characterize the disturbed zone, which will necessarily rely on the Mohr-Coulomb model.

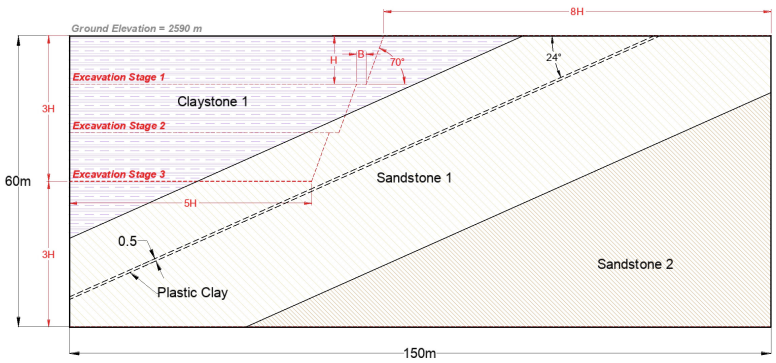

Fig. 1. The geological model represents a three-layered rock mass, with an additional layer of weak plastic clay.

Table 1. Geomechanical properties of materials included in the model.

Layer Name	Unit Weight (KN/m^3)	Cohesion (MPa)	Internal Friction Angle (degrees)	Elasticity Modulus (MPa)	P-Wave Velocity (m/s)	Poisson ratio
Claystone 1	21.9	0.109	32.2	1660	2850	0.35
Sandstone 1	20.8	0.148	37.6	1480	3380	0.32
Sandstone 2	23.1	0.187	40.4	2920	3920	0.30
Plastic Clay	20.2	0.030	26.8	0.60	1080	0.40

3 Initial Field Monitoring

3.1 Geotechnical Monitoring Data Before the Disturbance of the Medium

During the subsoil exploration activities for the mining project, a plastic clay thin-layer was discovered, prompting an early advisory of potential slope instability issues. As a precautionary measure, the installation of an inclinometer was suggested, as well as the calibration of a numerical model to track ground horizontal deformations at specific depths.

The inclinometer results indicate the horizontal displacements at various depths. In this case, a particular section of the instruments was showing significant displacement at 24.5 m' depth, corresponding to the depth of the thin plastic clay layer at the site, which was identified early in the project, before the open pit excavations started.

Simultaneously with the field monitoring, a numerical model was built to keep control on the deformations that would be expected in the excavation. The model was run at the end of every excavation stage, and results of horizontal deformation were compared against the results from the field monitoring, which are the inclinometer data presented above.

The main idea with the numerical model was to calibrate the elastic and plastic properties of the thin layer of plastic clay, so by forcing the model to get similar horizontal displacements to those measured in the field monitoring, it was possible to see how the properties in the plastic would be different from the ones considered at the beginning (see Table 2), which means the material was changing its shear strength with deformation and that consideration is not included in the numerical model. An example of horizontal displacements results obtained from the numerical model, using the finite elements method, is presented in Fig. 2.

4 Disturbance of the Medium Using Controlled Blasting

4.1 Geometry of the Disturbed Zone

The geometry of the disturbed zone inside the medium was defined by the distribution of the blasting holes, the radius of the fragmented zone expected by each blasting hole (B), and the total length of the disturbed zone, which was experimentally increased from

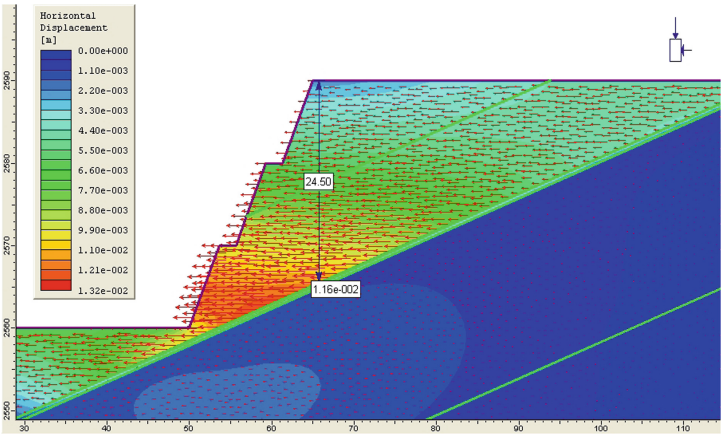

Fig. 2. Results from Finite Element Model – Stage 3: horizontal displacement at 24.5 m was predicted to be 11.6 mm.

Table 2. Horizontal displacement: comparison of field monitoring results and FEA model

Excavation Stage	H $_{Disp.}$ Field Monitoring (mm)	H $_{Disp.}$ FEA Model (mm)	Difference (%)
Stage 1	2.31	2.26	2.16
Stage 2	5.74	5.60	2.43
Stage 3	14.64	11.60	20.76

0.5H until 2.0H, when a change in the trend of deformations inside the medium was detected in the field monitoring. A complete diagram of the expected disturbed zone is presented in Fig. 3.

It is anticipated that extremely hard but brittle rocks will fracture easily, whereas soft elastic rocks will not break into small pieces, but they will be just fragmented into some bigger blocks [1]. In addition, the primary force causing movement of rock fragments is perpendicular to the axis of the holes, and when the holes are inclined according to the inclined strata, it is expected that the material will be pushed downward into the plastic clay.

There are various methods to estimate the radius of the affected area around a blasting hole, which refers to the region where rock fragmentation occurs after blasting. To accurately determine this radius, denoted as B, it is important to acknowledge the primary hypothesis that when a blasting compression wave propagates from a medium of higher impedance to one of lower impedance, some energy is reflected as a tension wave, resulting in the fracturing of the higher impedance medium. [1].

In this study, the impedance ratio between the “Sandstone 1” and the “Plastic Clay” is about 3.2, which means once the blasting energy reached the boundary between these two materials it will be partially reflected into tension waves that will break the rock

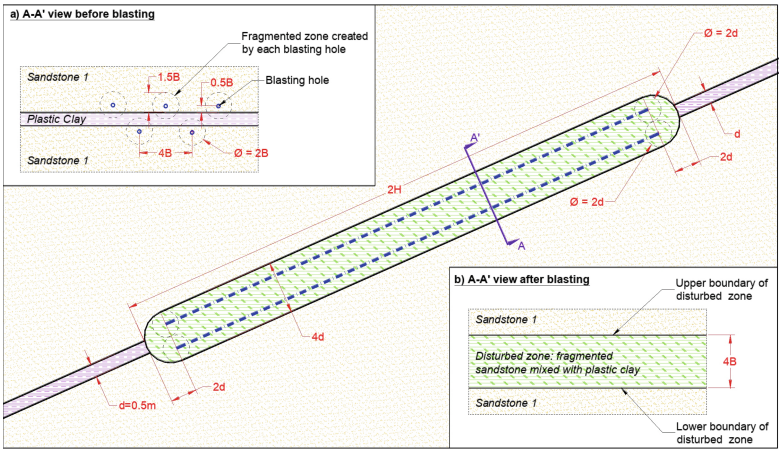

Fig. 3. Geometry of the disturbed zone: the distribution of the blasting holes is also presented, as well as the dimensions of the fragmented radius (B)

"Sandstone 1". The distance between the aforementioned boundary and the blasting hole is known as the burden, which could be estimated to be half the fragmentation radius (B). Thus, the blasting holes were defined to be drilled parallel to the interface with the "Plastic Clay" and separated an offset of 0.5B. (see in Fig. 3).

The following formulation could be used to estimate the minimum burden B in underground blasting when using diameters (D) up to 165mm for the blasting hole [1]:

$$B = 11.8D^{0.63} \tag{4}$$

The diameter of the blasting holes was 2.5 inches (63.5mm), and the estimated burden was close to 2.0m in this case. To fracture both the rock layer above and below the plastic clay layer, the blasting holes were staggered and the blasting power reduced by half. Consequently, the calculated burden had to be adjusted by a factor of 0.5, resulting in a final B value of approximately 0.5m, which is comparable to the thickness of the plastic clay layer.

4.2 Characterization of the Disturbed Zone

To characterize the disturbed zone, which corresponds to a mixture of sandstone rock blocks within a plastic clay, the approach proposed by Nikolaidis & Saraglou [7] was adopted. This approach was proposed for the characterization of "bimrocks," or bloc-in-matrix rocks, and involves the use of stereological analysis to extrapolate one-dimensional or two-dimensional data and estimate the volumetric proportion of the rock blocks.

Estimating the spatial distribution of the blocks inside these geological materials is a challenging task due to their complex and chaotic nature, which makes it difficult to employ a simplistic approach. Additionally, the complexity of these materials and the challenges associated with their sampling during ground investigations often lead to a

lack of high-quality laboratory and in-situ testing data. For these reasons, the approach proposed by Nikolaidis & Saraglou [7] has been used to deal with "bimrocks" for the past two decades.

The parameters needed to characterize the "bimrocks" in this case are listed next:

1. Characteristic engineering dimension: in this study it was adopted to be 0.75, (maximum distance expected for the fractured zone to extend).
2. Block to matrix volume proportion: based on the geometry of the disturbed zone, the proportion between rock blocks and plastic clay matrix is 75% to 25%, respectively.
3. Block to matrix shear strength proportion: based on the properties presented in Table 1, the rock blocks are to have a significantly higher shear strength than the plastic clay. (Cohesion for the plastic clay is 80% lower than the value for the block rocks; internal friction angle for the plastic clay is 28% lower than the value for the block rock).
4. Blocks orientation was considered chaotic because the blocks are generated by blasting the rock mass.

The cumulative "bimrock" strength (CBS) is estimated following this equation [7], where UCS is the unconfined compressive strength:

$$CBS = \frac{Block\ Proportion}{100\%} \times UCS_{Blocks} + \left(\frac{Matrix\ Proportion}{100\%} \times UCS_{Matrix} \right) \quad (5)$$

Now, in order to use the Mohr-Coulomb model, the shear strength of the materials was evaluated in this project using cohesion and internal friction angles. Thus, it is necessary to propose a modification of the equation proposed by Nikolaidis & Saraglou [7], in order to get a weighted cohesion and internal friction angle to characterize the material in the disturbed zone. These are the proposed equations:

$$c'_{CBS} = \frac{Block\ Proportion}{100\%} \times c'_{Blocks} + \left(\frac{Matrix\ Proportion}{100\%} \times c'_{Matrix} \right) \quad (6)$$

$$\phi'_{CBS} = \frac{Block\ Proportion}{100\%} \times \phi'_{Blocks} + \left(\frac{Matrix\ Proportion}{100\%} \times \phi'_{Matrix} \right) \quad (7)$$

The same approach was followed to obtain other parameters like unit weight, elasticity modulus, P-wave velocity and Poisson's ratio.

Table 3. Geomechanical properties of materials in the disturbed zone

Layer Name	Unit Weight (KN/m^3)	Cohesion (MPa)	Internal Friction Angle (degrees)	Elasticity Modulus (MPa)	P-Wave Velocity (m/s)	Poisson ratio
Bimrock (disturbed zone)	20.35	0.060	29.5	370.5	1655	0.38

5 Slope Stability Analysis

Upon comparing the inclinometer results for horizontal displacements at a depth of 24.5 m, it became evident that the model did not accurately reflect the deformation behavior of the thin layer. The engineers responsible for the mining excavation proposed a solution by using explosives in the sandstone layers immediately above and below the plastic clay layer. This technique, previously employed in similar mining operations, aims to eliminate the continuity of the thin weak layer by breaking the surrounding rock and mixing it with the plastic clay. As a result of this technique, a portion of the medium would have blocks of rock embedded in a plastic matrix. It is anticipated that the disturbed zone would possess greater shear strength parameters compared to the plastic clay layer alone.

5.1 Limit Equilibrium vs. Finite Element Results: Before the Disturbance of the Medium

Initially, the slope stability assessment was done by using the limit equilibrium method (i.e. Bishop simplified, GLE/Morgenstern-Price, Spencer) and then compared with the result from the numerical model simulations using the finite element analysis technique (i.e. strength reduction factor method). The results comparison is presented in the following Table 4 for static analysis, and Table 5 for pseudostatic analysis.

Based on the previous findings, two main observations can be made. Firstly, the Factor of Safety obtained through the strength reduction method is consistently lower than that obtained through the limit equilibrium method. Secondly, when considering

Table 4. Factor of Safety (FoS) for static analysis using Limit Equilibrium Method (LEM) and Finite Element Analysis (FEA) with the strength reduction factor (SRF).

Excavation Stage	FoS LEM (Bishop)	FoS LEM (GLE/M-P)	FoS LEM (Spencer)	FoS FEA_{SRF} (static)
Stage 1	3.21	3.36	3.38	3.26
Stage 2	2.46	2.47	2.46	2.32
Stage 3	1.51	1.50	1.50	1.42

Table 5. Factor of Safety (FoS) for pseudostatic analysis using Limit Equilibrium Method (LEM) and Finite Element Analysis (FEA) with the strength reduction factor (SRF).

Excavation Stage	FoS LEM (Bishop)	FoS LEM (GLE/M-P)	FoS LEM (Spencer)	FoS FEA_{SRF} (pseudostatic)
Stage 1	2.58	2.57	2.57	2.62
Stage 2	1.96	2.11	2.03	1.88
Stage 3	1.03	1.05	1.17	0.96

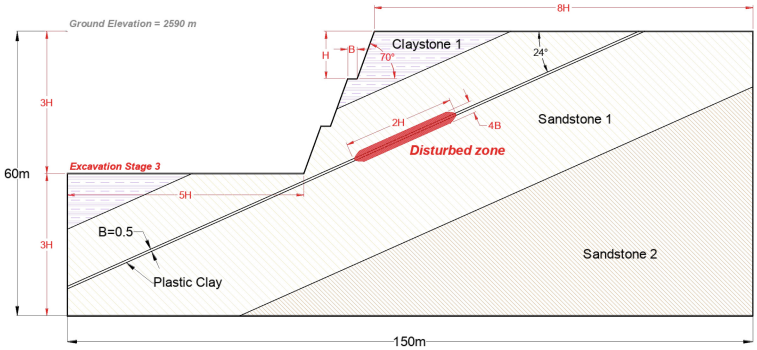

Fig. 4. The geological model represents a three-layered rock mass, with an additional layer of a weak plastic clay and rather modified to include a disturbed zone.

the pseudostatic scenario, for stage 3, the factor of safety obtained from the strength reduction method falls below 1.0, which is not recommended for safe mining operations. Moreover, it is important to note that monitoring results indicate that the horizontal displacements observed in the field were greater than those predicted by the numerical model (FEA_{SRF}). This implies that the actual factor of safety in the field may be even lower than the predicted values obtained through the strength reduction factor technique.

These results were crucial for mining excavation engineers to determine whether to utilize explosives to create a strip of fractured rock, such that the continuity of the weak layer would be discontinuous by intervening in the thin layer of plastic clay.

5.2 Limit Equilibrium vs. Finite Element Results: After the Disturbance of the Medium

The suggested approach involved blasting a section within the rock mass that was adjacent to the narrow weak layer and approximately 20 m in length. This method would create a strip of rock fractured by explosives, which comprises a combination of mixed materials, including rock blocks and plastic clay, which would effectively break the continuity of the weak layer. The new geometry for the geological geomechanical model is presented in Fig. 4.

The parameters to characterize the strip of rock fractured by blasting (disturbed zone), were presented in Table 3. The new results for slope stability are presented in Table 6 for static conditions and in Table 7 for pseudostatic conditions, which consider the model after the disturbance of the medium. The results from FEA showing the maximum shear strain in the pseudostatic condition are presented in Fig. 5.

6 Final Field Monitoring

6.1 Geotechnical Monitoring Data After the Disturbance of the Medium

The method's effectiveness was confirmed through ongoing inclinometer monitoring following the disturbance of the medium. The results, depicted in Fig. 6, indicate a shift in displacement trends at a depth of 24.5 m. This change in trend is likely attributable to

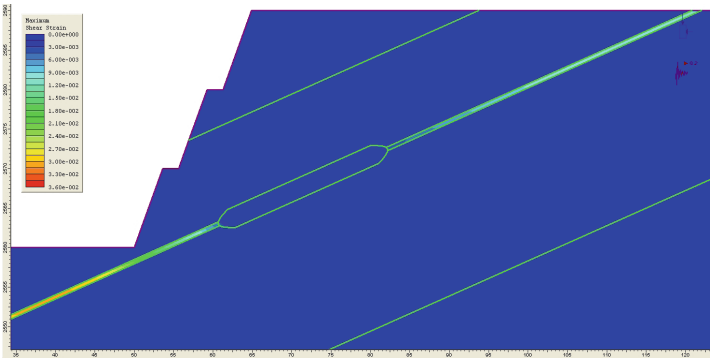

Fig. 5. Results from Finite Elements Method – Stage 3: maximum shear strain in pseudostatic condition after the disturbance of the medium.

Table 6. Stage 3 after the disturbance of the medium: Factor of Safety (FoS) for static analysis using Limit Equilibrium Method (LEM) and Finite Element Analysis (FEA) with the strength reduction factor (SRF).

Excavation Stage	FoS LEM (Bishop)	FoS LEM (GLE/M-P)	FoS LEM (Spencer)	FoS FEA_{SRF} (static)
Stage 3 (disturbed zone)	1.60	1.68	1.72	1.42

Table 7. Stage 3 after the disturbance of the medium: Factor of Safety (FoS) for pseudostatic analysis using Limit Equilibrium Method (LEM) and Finite Element Analysis (FEA) with the strength reduction factor (SRF).

Excavation Stage	FoS LEM (Bishop)	FoS LEM (GLE/M-P)	FoS LEM (Spencer)	FoS FEA_{SRF} (pseudostatic)
Stage 3 (disturbed zone)	1.14	1.14	1.27	1.04

the disturbance of the medium, intervention that took place on day 236 of the project (it should be mentioned that the excavations of the stage 1 started on day 180 of the project). Prior to day 236, the displacements displayed a distinct trend towards failure, with displacement rapidly increasing. However, following the disturbance of the medium, which involved creating a strip of fractured rock embedded in the plastic clay matrix, the displacement trend changed and began to stabilize.

7 Conclusions

In this paper, a solution is proposed for stabilizing a slope in a mining open pit that is characterized by a rock mas with a thin and weak layer of plastic clay. The use of field monitoring data and a calibrated numerical model initially showed that the use of blasting

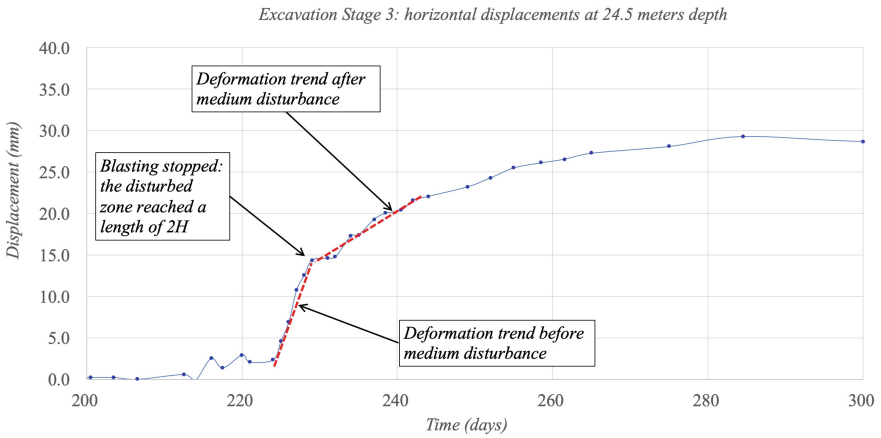

Fig. 6. Results of field monitoring: blasting was stopped when the disturbance of the medium reached a total length of 2H on day 236, which showed a change in the horizontal displacements' trend.

to disturb the rock mass surrounding the weak layer is an effective way to improve the slope stability in open pits. In this case, the benefit of employing numerical simulation with finite element analysis is the ability to calculate displacements and then compare them to field measurements. After detecting the potential for failure in the slope, by using the finite element numerical model's shear strength reduction analysis results, it became feasible to suggest a disturbance of the medium to increase the factor of safety and mitigate the probability of failure.

The field monitoring was fundamental to identify the deformations' trend before the rock mass blasting was implemented to disturb the medium. Moreover, the field monitoring allowed a daily control to evaluate the effectiveness of the rock blasting, which was progressively increasing the total length of the disturbed zone. Once the deformations trend changed, it was concluded the rock blasting could be stopped.

The use of field monitoring data was crucial, to understand that before day 236 there was a clear tendency for displacements to increase rapidly, indicating a trend towards failure. However, after the disturbance of the medium, which consisted in fragmenting the sandstone rock to generate a strip of fractured rock into the plastic clay matrix (a bimrock [7]), a new estimation of shear strength parameters was done to re-evaluate the stability of the slope.

Acknowledgement. The University of Waterloo is acknowledged by the author for providing support that enabled the use of the software during his time as a PhD student.

References

1. Alonso, J. B., Gómez, J. C., & Herbert, J. H. (2013). Perforación y voladura de rocas en minería. Universidad Politécnica de Madrid: Madrid, Spain.
2. Crusoe Jr, G. E., Cai, Q. X., Shu, J. S., Han, L., & Barvor, Y. (2016). Effects of weak layer angle and thickness on the stability of rock slopes. International Journal of Mining and Geo-engineering, 50(1), 97-110.
3. Hammouri, N. A., Malkawi, A. I. H., & Yamin, M. M. (2008). Stability analysis of slopes using the finite element method and limiting equilibrium approach. Bulletin of Engineering Geology and the Environment, 67, 471-478. https://doi.org/10.1007/s10064-008-0156-z
4. Hoek, E., Carranza-Torres, C., & Corkum, B. (2002). Hoek-Brown failure criterion-2002 edition. Proceedings of NARMS-Tac, 1(1), 267-273.
5. Kim J., Salgado, R., & Yu H. (1999) Limit analysis of soil slopes subjected to pore-water pressures. J Geotech Geoenviron Eng ASCE 125(1):49–58
6. Lane, P., Griffiths, D. (2000) Assessment of stability of slopes under drawdown conditions. J Geotech Geoenviron Eng ASCE 126(5):443–450
7. Nikolaidis, G., & Saraglou, C. (2016) Engineering Geological Characterisation of Block-In-Matrix Rocks. Bulletin of the Geological Society of Greece, vol. L, p. 874–884. Proceedings of the 14th International Congress, Thessaloniki, May 2016.
8. Rocscience Inc. (2001) Application of the finite element method to slope stability, Toronto.
9. Zaki, A. (1999) Slope stability analysis overview. University of Toronto